ELSEVIER

Polymer 42 (2001) 5425–5437

polymer

www.elsevier.nl/locate/polymer

Creep damage mechanisms in polyethylene gas pipes

H.B.H. Hamouda[a], M. Simoes-betbeder[a], F. Grillon[a], P. Blouet[b], N. Billon[c], R. Piques[a,*]

[a]*Centre des Materiaux Pierre-Marie Fourt, Ecole des Mines de Paris, CDM-UMR CNRS 7633, BP 87, 9100 Evry, France*
[b]*Gaz de France, D.R. DRX-La Plaine, Saint Denis, France*
[c]*Ecole des Mines de Paris, CEMEF-UMR CNRS 7635, Sophia-Antipolis, France*

Received 18 June 1999; received in revised form 21 September 1999; accepted 14 June 2000

Abstract

This study deals with the creep damaging processes of two polyethylene (PE) resins. One is a ductile material while the other is a brittle one. Scanning electron microscopic (SEM) observations as well as chemical analysis are used to identify elementary process involved in the crack initiation and propagation. Of the two considered resins, only the second exhibits a lifetime controlled by slow crack growth (SCG). It is shown that catalytic residues act as initiating agents for the damage. Nevertheless, the presence of such particles in an extruded resin does not lead to a creep damage in every case.

Intraspherulitic micro-cracks (mirror zones) can then propagate. Propagation takes place between the lamellae, seemingly through a disentanglement of tie molecules connecting the lamellae. The orientation of the micro-cracks is perpendicular to the largest principal stress. Cryogenic fracture surfaces indicate that the mirror zone gives rise to discontinuous crack growth bands (DCGB). In a pre-cracked specimen, only the DCGB stage takes place in the crack tip. © 2001 Published by Elsevier Science Ltd.

Keywords: Polyethylene; Creep damage; Slow crack growth

1. Introduction

Two types of polyethylene (PE) used for extruded gas pipes are presented in this study. The first one fails as a creep ductile material when the loading is overestimated. Conversely, the second exhibits a brittle behavior. Nowadays, pipe networks for gas supply, mostly involve this latter kind of creep brittle material for which the failing mode is slow crack growth (SCG).

Slow crack propagation in PE has a considerable practical importance since it occurs at low stresses and can induce long-term failure in engineering components. An accurate method for predicting this type of fracture should be based on the understanding of the basic mechanisms involved. This paper deals with these mechanisms, i.e. the damaging processes of such PE in order to accurately predict the pipe lifetime.

In this type of material, low apparent stresses (i.e. lower than yield stress) induce brittle fracture after a more or less long incubation period. Damages are assumed to appear and grow during this step. Our purpose is to identify the nature, the location and the mechanical effect of these damages in PE resins.

Many authors have reported in the past on this kind of brittle rupture initially using environmental stress cracking (ESC) agents [1,2]. In a second step, experiments in air [3] have been performed. The fibrous aspect of the fracture surface suggests the existence of a craze at the tip of the crack in a previous stage of the rupture. Transmission electron microscopy confirms this point as void structures which can be observed at the tip of a crack [4].

To promote SCG failures in short time, adapted to laboratory conditions, many different techniques were used. One of these is the three-point bending test developed by the Gas Research Institute [5]. This technique, together with the observation of the fracture surface revealed that the SCG process is discontinuous, consisting of rather abrupt crack extensions followed by arrests. These discontinuities or arrest lines were also described by Chan and Williams [2] and referred to as a "stick-slip mechanism". This phenomenon is associated with crack blunting. Lustiger and Corneliussen [6] and Lu and Brown [7] also noticed arrest lines in PE and suggested the use of Dugdale theory [8] to model such behavior.

At a microscopic level, and in the presence of an ESC agent, Singleton et al. [1] stated that crack propagation should be interlamellar due to a lubrication (see e.g. Ref.

* Corresponding author.

0032-3861/01/$ - see front matter © 2001 Published by Elsevier Science Ltd.
PII: S0032-3861(00)00490-0

Table 1
Properties of resins used in the tested PE pipes

Resin	Comonomer	ρ (g/cm^3)	MI (5 kg)	M_n	M_w	M_z	SCB (1000C)
A	Hexene	0.940	0.9	11 900	115 700	440 200	6.245
B	Butene	0.949	0.7	23 100	151 300	640 000	7.380

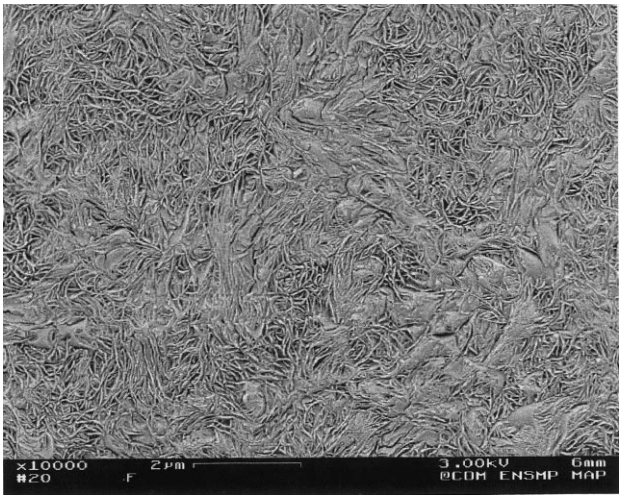

Fig. 1. Semi-crystalline microstructure (resin A).

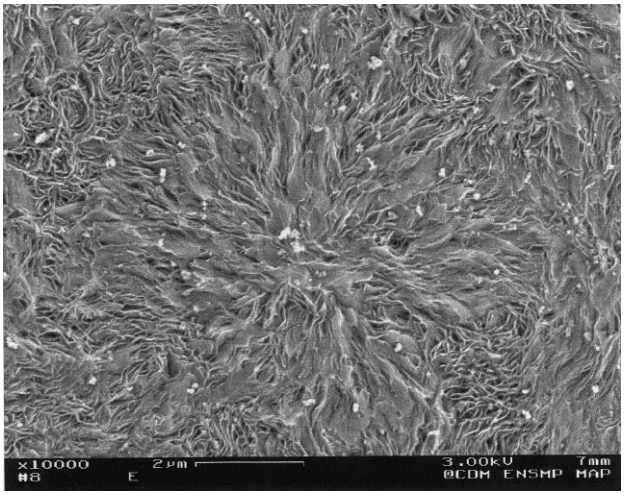

Fig. 2. Spherulitic microstructure (resin B).

[9] of the amorphous material connecting the crystals. The diffusion of an ESC agent in the resin should accelerate the fracture and create secondary crazes by weakening the cohesion between the drawn fibrils.

However, this kind of failure can be observed even in air (i.e. without ESC) as shown in the present paper. Additionally, the present work deals with the comparison between notched and unnotched samples and tubes, and aims to enlighten us on the main factors controlling creep damage mechanisms.

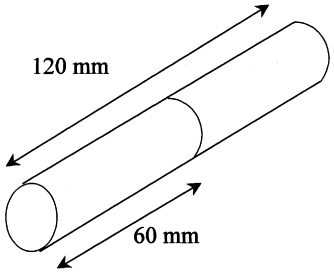

Fig. 3. Schema of full notched crack tensile (FNCT) specimen.

2. Experimental procedure

The specimens are tooled from commercial 110 mm outer diameter gas pipes with a 10 mm thick wall. Two PEs are used (Table 1); one, referred to as A, is a ductile resin (in the explored experimental domain) and the second, referred to as B, exhibits a brittle failure during creep tests.

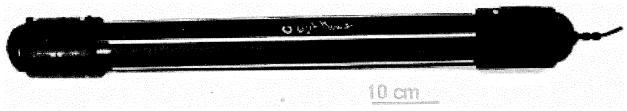

Fig. 4. Sample of pipe used in creep test under hydrostatic pressure at 180°C.

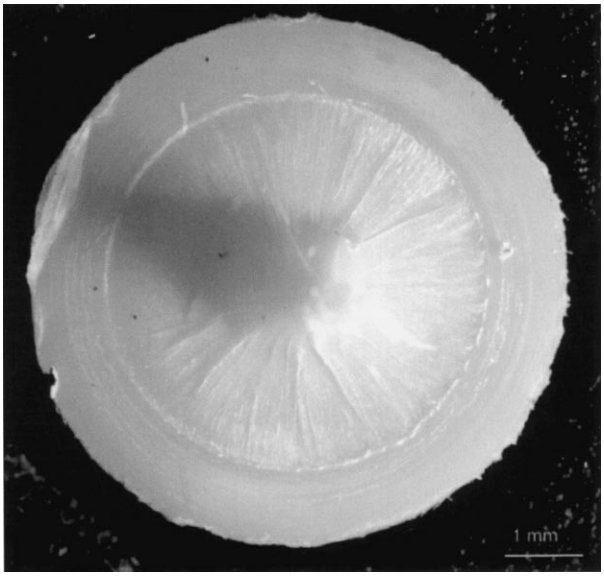

Fig. 5. Ductile fracture surface: FNCT creep failure at 60°C under 8 MPa (resin A).

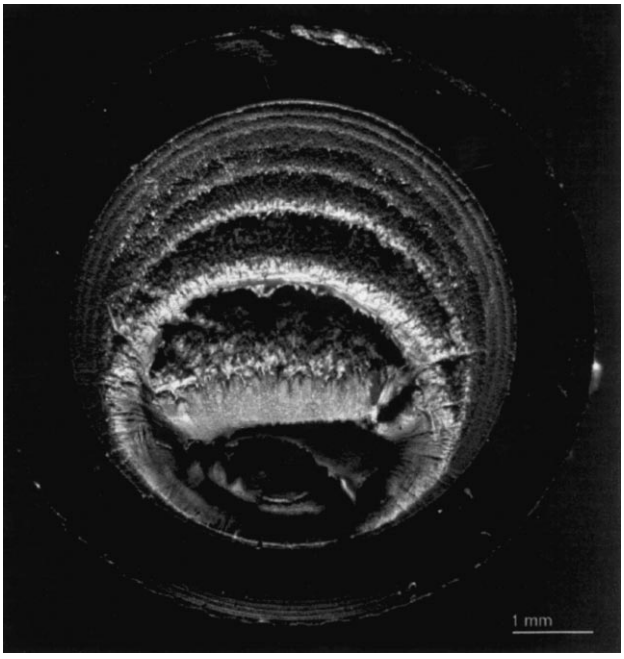

Fig. 6. Brittle fracture surface: FNCT creep failure at 60°C under 5 MPa (resin B).

To perform scanning electron microscopic (SEM) observations, samples are first cold microtomed and then etched in a specific chemical solution (sulfuric acid, phosphoric acid and water). SEM observations are made after coating samples with gold–palladium. By this procedure it is possible to discriminate crystalline ribbon from amorphous regions as well as to observe stable crazes and voiding resulting from mechanical loading.

Both the resins exhibit an initial semi-crystalline microstructure composed of more or less perfect spherulites (Figs. 1 and 2). The spherulites are better defined and bigger in resin B (Fig. 2).

Mechanical tests are performed using two types of specimens:

Notched specimens are full notched creep tensile (FNCT) specimens tooled from a gas pipe wall. Their diameter is 8 mm (Fig. 3). The samples are extracted parallel to the extrusion direction. The notch is made using a fresh razor blade. Its depth is 1 mm. The experiment consists of the measurement of the displacement of the loading point (using precise extensometer) and of the applied tensile force as a function of time. The time for complete failure is also recorded. The scatter in the load point displacement measurements is within ±15%. The tests are conducted at 40, 60 and 80°C with a temperature tolerance of ±1°C. The constant applied stress is calculated with respect to the notched cross-section. The crack tip damage zone is observed (using SEM analysis) on specimens cut parallel to a meridian plane of the sample. The fracture surface is also observed.

Table 2
A summary of FNCT creep tests for resins A and B (b, brittle creep failure; d, ductile creep failure)

	40°C			60°C					80°C		
Stress (MPa)	10	12	14	5	7	8	9	10	5	6	7
A	d	d	d			d	d	d	d	d	d
B	b	b	d	b	b	b	b	d	b	b	d

Unnotched specimens are 1 m long gas pipe portions, clamped at their ends and creep tested under a hydrostatic pressure of 9.6 bar at 80°C (Fig. 4). A leak of water due to the initiation and the propagation of a creep crack through the pipe wall generally limited the lifetime. Small arc-shaped specimens are then cut from the cross-section of these pipes and fractured in liquid nitrogen. In the brittle fracture surface, the SEM observations show the creep damaged zones.

3. Results

3.1. Creep crack testing

In the case of FNCT specimens, the presence of a crack induces a stress concentration in the vicinity of the crack tip and causes the structure to fail. Table 2 summarizes the obtained results.

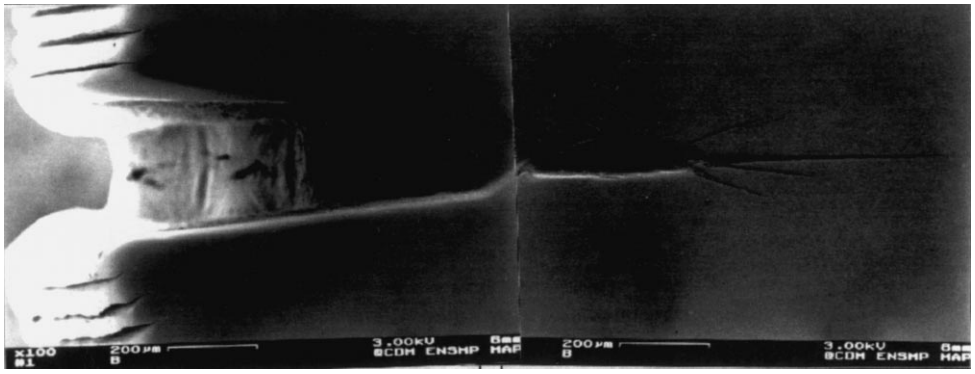

Fig. 7. Creep damage at the crack tip: "ϵ" shape crack (side view of FNCT specimen tested at 60°C under 8 MPa, resin B).

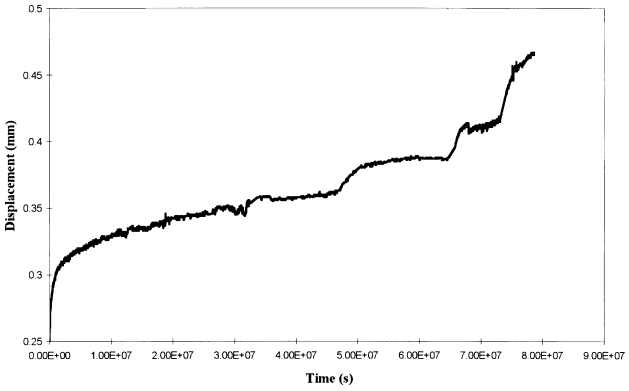

Fig. 8. FNCT creep test at 60°C under 5 MPa (resin B).

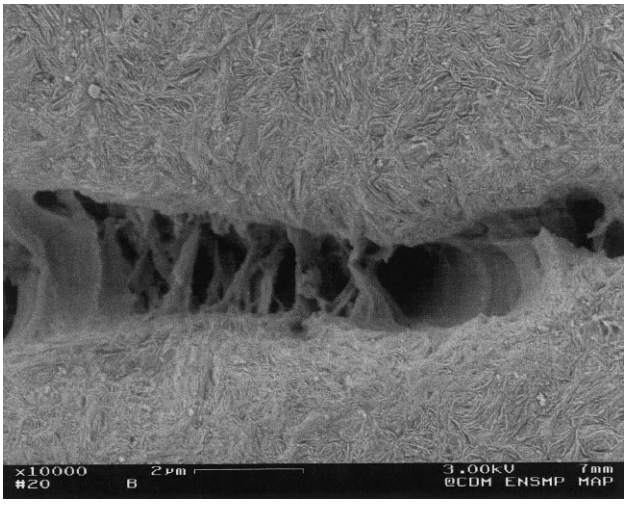

Fig. 9. Microstructure of the principal craze after etching (resin B).

Fig. 10. Microstructure of a secondary craze after etching (resin B).

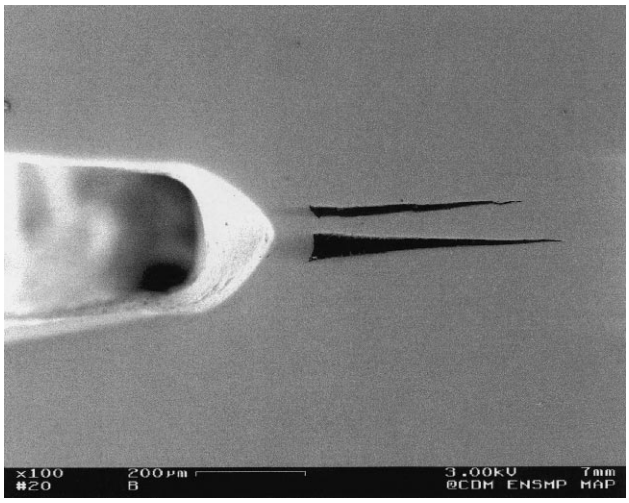

Fig. 11. Initiation of creep damage at the crack tip: side view of FNCT specimen tested at 60°C under 8 MPa (resin B after etching).

Fig. 12. Ductile failure under hydrostatic pressure (9.6 bar) at 80°C (resin A).

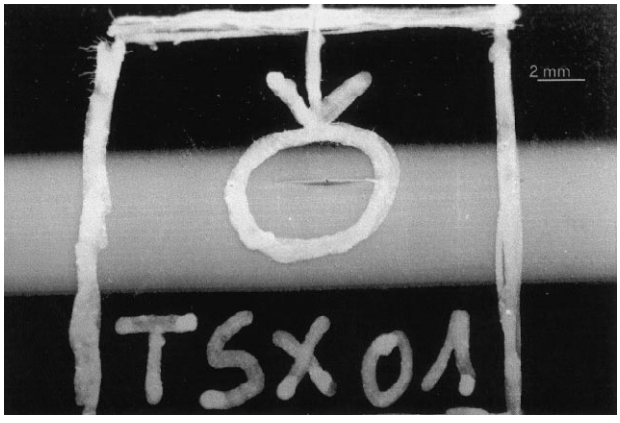

Fig. 13. Brittle failure under hydrostatic pressure (9.6 bar) at 80°C (resin B).

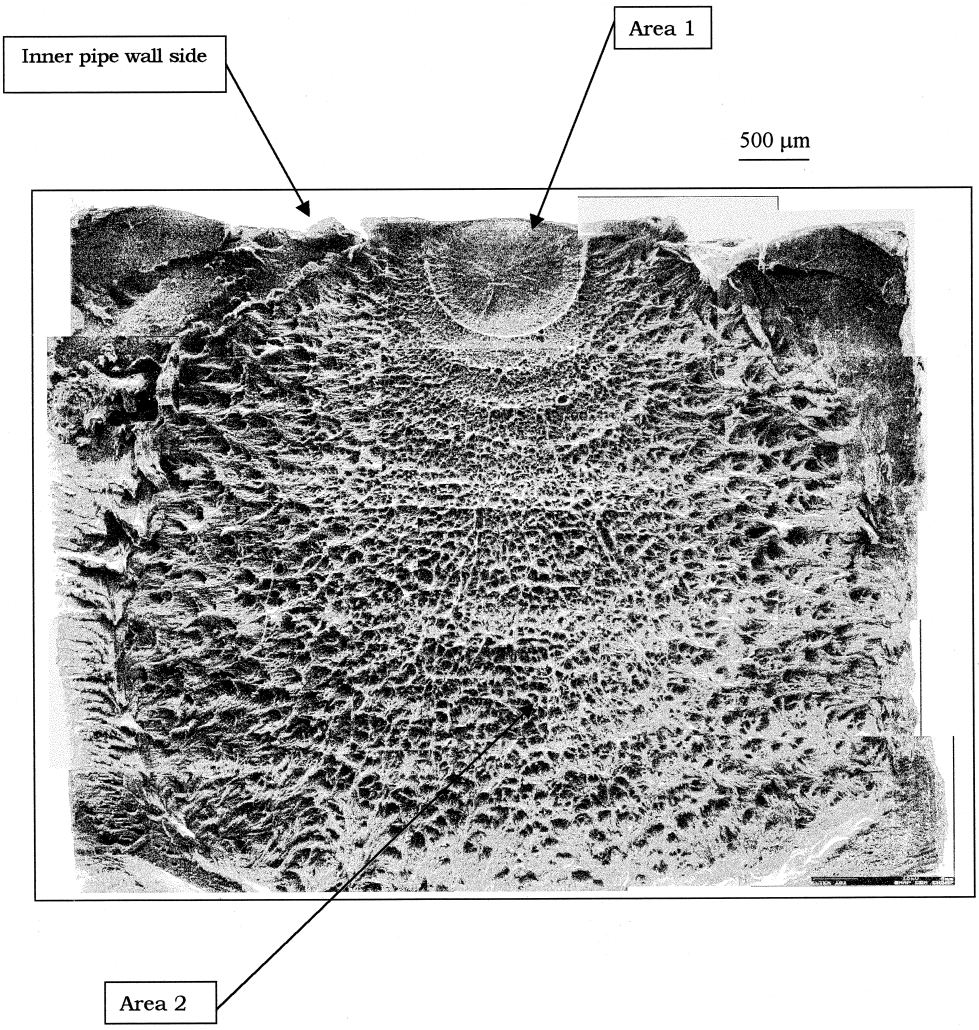

Fig. 14. Brittle fracture surface: gas pipe creep failure (9.6 bar) at 80°C (resin B).

In the case of resin A, the failure is always ductile. The ductile fracture surface, which is essentially equivalent for all these tests, is shown in Fig. 5. Because of the presence of the notch, the deformation is localized in the crack plane. Then failure occurs for a creep which depends on the stress and the temperature.

In the case of resin B, the failure is brittle for low stress but ductile at higher stress. These kind of results have already been reported in the past by Lu and Brown [10] who observed a slow crack growth brittle to ductile mode transition at stresses of half of the yield stress. Our samples exhibit this latter type of behavior (Fig. 6 (top view) and Fig. 7 (side view)) consisting of discontinuous crack growth. Because of the high sensibility to the load point alignment, in Fig. 6 the failure pattern is "off-center". In Fig. 7, after etching, an epsilon crack shaped at the crack tip is observed. The fracture initiates within a craze growing from the root of the razor blade pre-crack and SCG process could be explained by a competition between the following two mechanisms:

- crazing process taking place in the zone where the highest principal tensile stress is induced by the crack;
- micro-shear banding at the notch root.

The interaction between these two mechanisms successively stops the crack propagation and causes SCG by discontinuous bands. Load point displacement as a function of time (Fig. 8) is a trace of such a phenomenon. Every jump in such a record should correspond to a forward step of the crack. The step depth increases with time. The first ones appear so tiny that the corresponding jumps are not detectable.

The microstructures of the principal (parallel to the pre-crack) and secondary crazes are shown in Figs. 9 and 10 after etching. It can be noticed that the deformation is very localized in these regions where many micro-fibrils appear. The main difference between these two regions is the direction in which the material is drawn. The cumulative

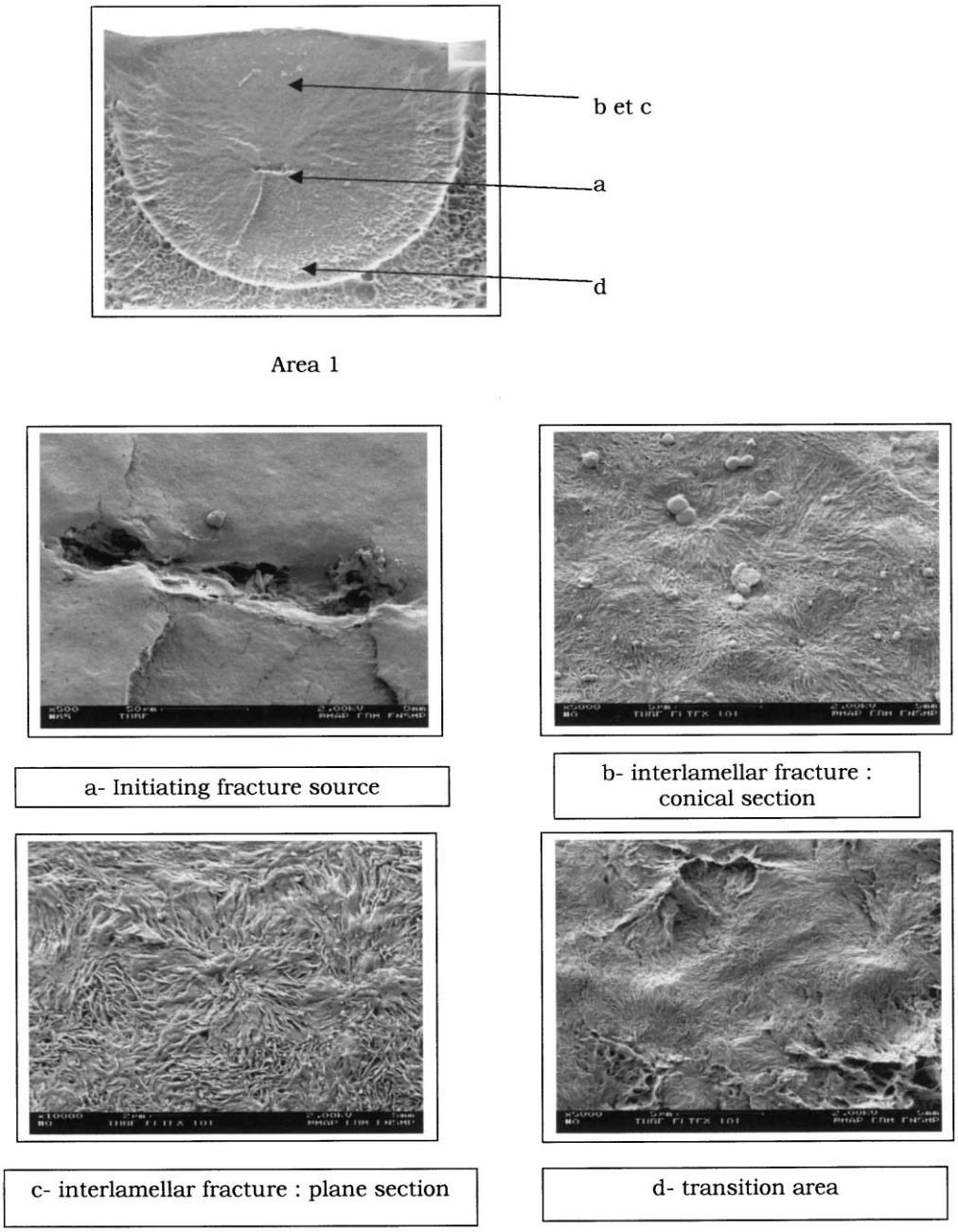

Fig. 15. Details of area 1: mirror zone (resin B). (a) Initiating fracture source. (b) Inter-lamellar fracture: conical section. (c) Inter-lamellar fracture: plane section. (d) Transition area.

effect of both shear and closure back the crack tip explain the orientation of the micro-fibrils in the zone of secondary crazes.

Initiation of crazes at the crack tip is not directly adjacent to the pre-crack (Fig. 11). The plain stress conditions in the crack tip induce a significant decrease of the yield stress. Therefore, this ligament is plastically deformed whereas the surrounding region is subjected to stress levels causing an initiation of SCG.

3.2. Continuum creep damage failure

In this case, samples are parts of gas pipes, and are not notched. Fracture occurs under hydrostatic pressure at 80°C.

Resin A breaks in a ductile manner after a localized deformation (Fig. 12).

Resin B is brittle. Creep crack initiates from the inner part and propagates through the pipe wall without visible deformation (Fig. 13). This involves widespread and significant creep damage ahead of the crack. Such continuum creep damage is illustrated in Figs. 14 and 15.

Fig. 14 shows a characteristic fracture surface of a SCG with a mirror zone (area 1) and discontinuous bands. The mirror zone (area 1) contains the initiating source of failure.

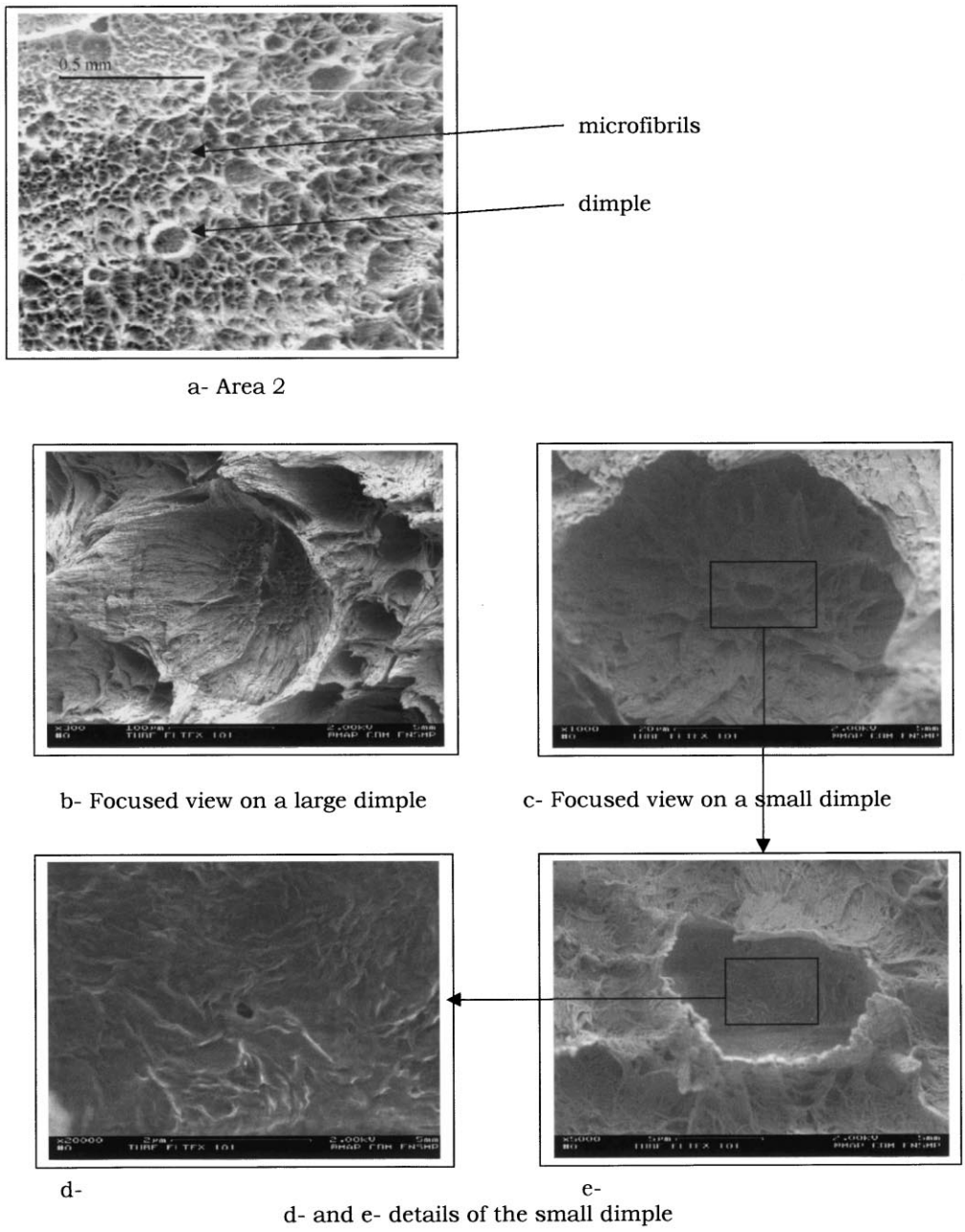

Fig. 16. Details of area 2: discontinuous growth bands (resin B). (a) Area 2. (b) Focused view on a large dimple. (c) Focused view on a small dimple. (d,e) Details of the small dimple.

Surrounding the mirror area, a transition zone with an increasing roughness initiates the beginning of the second stage, i.e. the propagation of the initial crack by discontinuous bands (area 2).

Fig. 15 shows details of the mirror area:

- Fig. 15a focuses on the initiating cavity of failure.
- Fig. 15b and c shows zooms of this smooth surface. We can distinguish spherulites and lamellae. No significant plastic deformation can be observed.
- Fig. 15d indicates the transition region where the fracture mechanisms change from an interlamellar process to a fibrillar one.

Fig. 16 shows the details of the fibrils in region 2, i.e. on the discontinuous growth bands. Many dimples and microfibrils (Fig. 16a and b) can be distinguished. Fig. 16c–e is successive focused views of a small dimple. Fig. 16e shows that the initiation of this damage is interlamellar.

Many other observations in the cross-section of the pipe creep tested at 80°C under hydrostatic pressure, reveal widespread short micro-cracks (10–70 μm) as shown in Fig. 17a. The orientation of the micro-cracks is perpendicular to the hoop stress in the tube. This damage initiates on a central cavity,

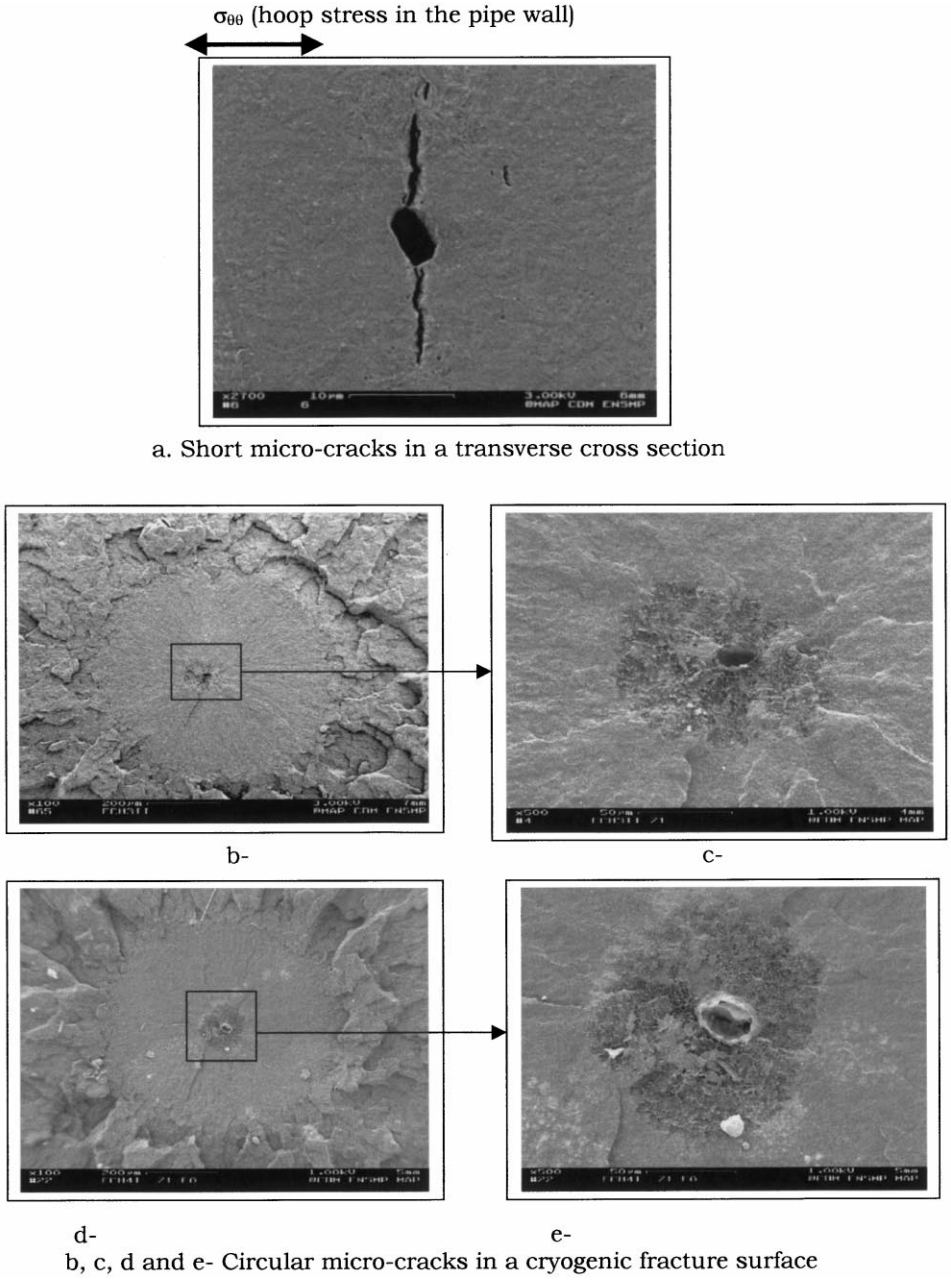

Fig. 17. Continuum creep damage in a pipe wall (resin B). (a) Short micro-cracks in a transverse cross-section. (b)–(e) Circular micro-cracks in a cryogenic fracture surface.

clearly evident in Fig. 17a. The feature of these micro-cracks are also revealed by cryogenic fracturing carried out on creep tested samples. Fig. 17b and c shows circular micro-cracks.

We have to pay more attention to the initiating source of creep failure for the mirror area (Fig. 15) and for the circular micro-cracks (Fig. 17). Fig. 18 roughly shows that fracture in this area should be interlamellar (Fig. 18a and b). In the center of each circular micro-crack, we can distinguish systematically a small cavity initiating the damage. All the observations gave similar results. Therefore, we can conclude that all the pipe wall volume is creep damaged as shown in Figs. 18 and 19.

Different zones could be distinguished (Fig. 18):

- a central cavity initiating the local failure (Fig. 18c–e);
- a fibrillated area similar to that observed after a slow crack growth surrounds this cavity (Fig. 18d and e); it corresponds to the first stage of propagation;
- the mirror area surrounding the previous one, results of micro-voids (Fig. 18a and c) and is the second seemingly interlamellar and intra-spherulitic stage of propagation.

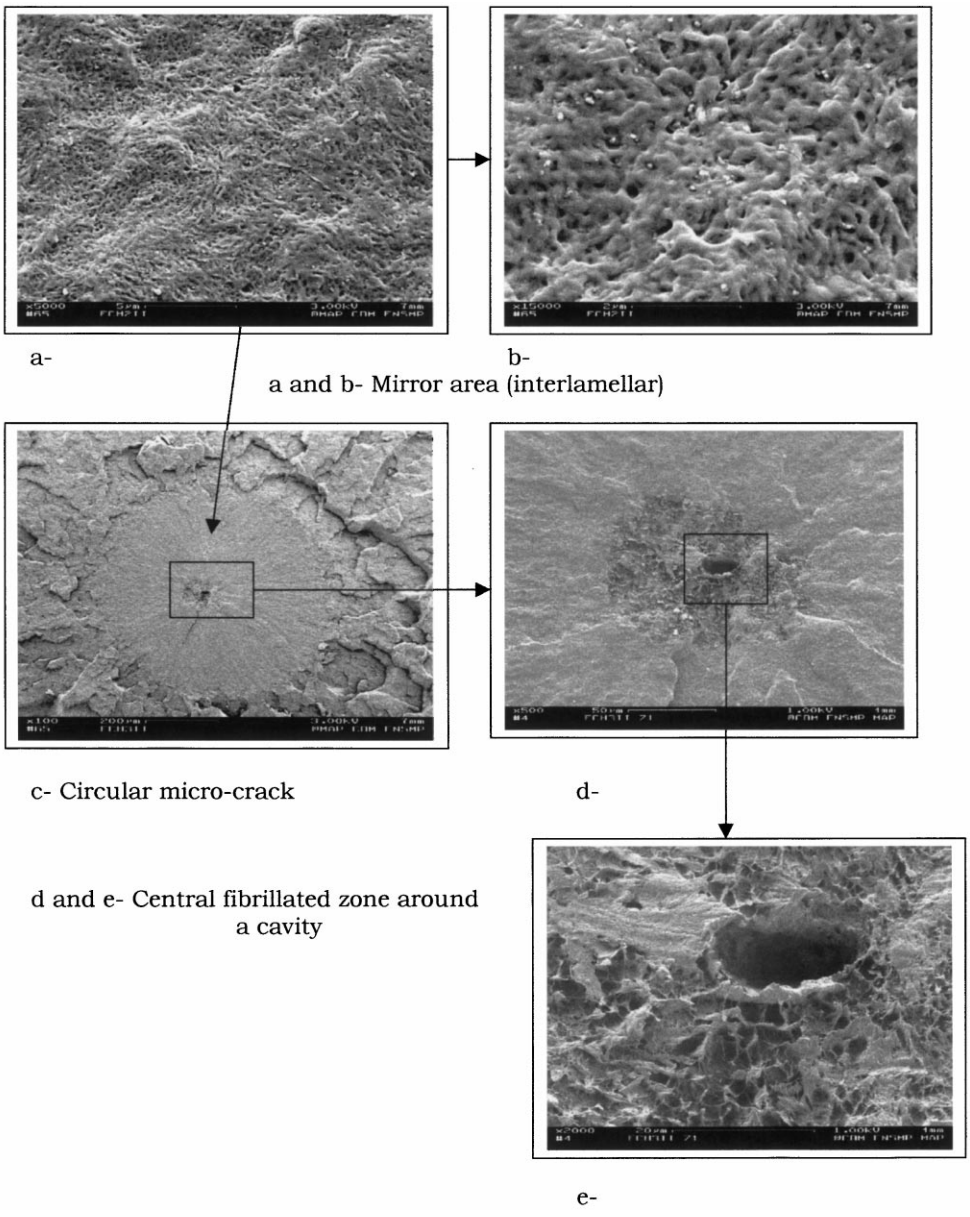

Fig. 18. The different creep damaged zones in a meridian cross-section of a pipe (resin B). (a,b) Mirror area (interlamellar). (c) Circular micro-crack. (d,e) Central fibrillated zone around a cavity.

When we emphasize the damaged region (Fig. 19), little particles can be distinguished in the center. Energy dispersive spectrometry (EDS) analyses of these particles reveal organo-metallic complexes with, in particular, the presence of titanium, aluminum and chlorine. These elements should be part of the components of a Ziegler–Natta type catalysis, and the particles should be catalytic residues.

Other analyses using X microprobe (wavelength dispersive spectrometry WDS) on microtomed samples (Fig. 20) show that the resin contains many particles of the same type (see Fig. 21).

In Figs. 15c,d and 18a,c we pointed out the interlamellar character of the mirror zone. Microtoming and etching make it possible to clearly confirm this assumption.

Fig. 22a and b shows intra-spherulitic propagation of micro-cracks with very little deformation. In the first case (Fig. 22a), the crack direction is deviated to a diagonal direction, after having reached the spherulite center. In the second case, the crack goes through the spherulite without deviation. These observations confirm that propagation is inter-lamellar and intra-spherulitic as we could think when focusing on the mirror area.

4. Discussion

4.1. Initiation of creep damage cracking

Many authors studied the initiation of damage in PE, and

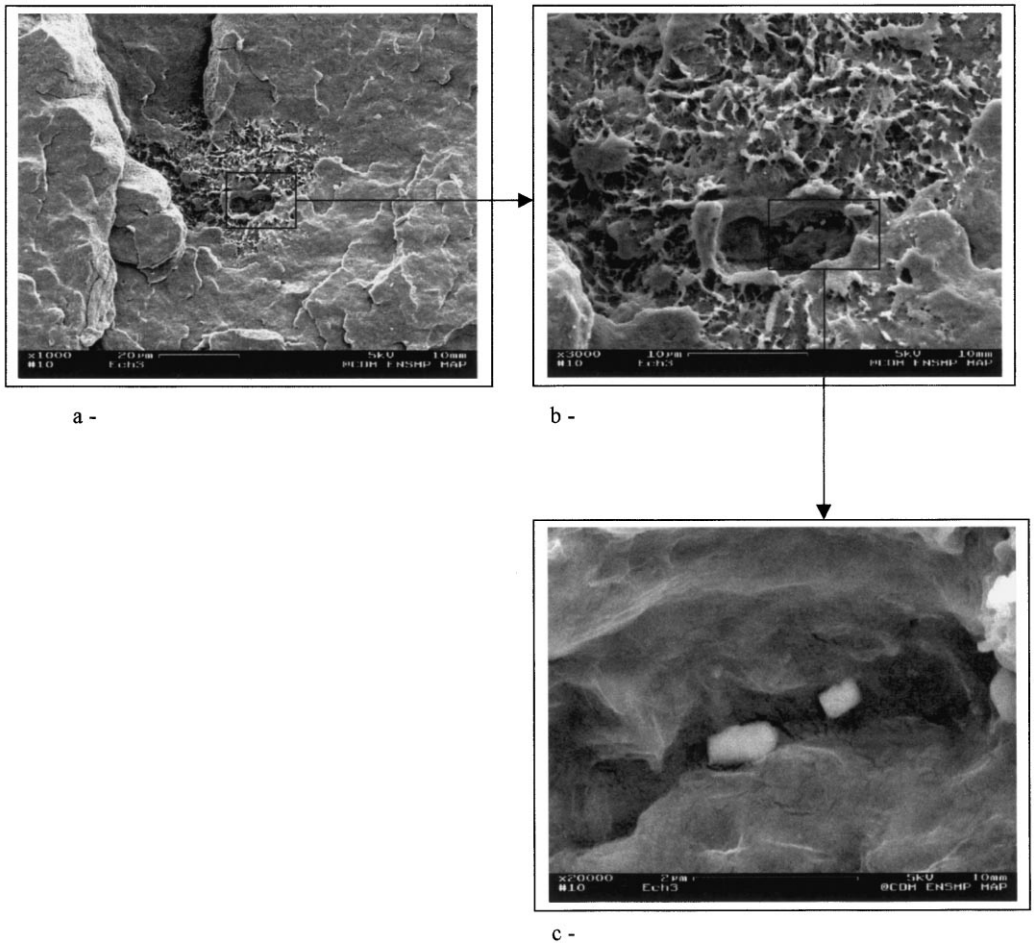

Fig. 19. Initiation of creep damage (resin B). (a,b) Central fibrillated zone around a cavity. (c) Catalytic residues particle inside the creep cavity.

explained this phenomenon by many types of defects in the resin. Stockmayer [11] for example, worked on PE creep properties, and concluded that creep cracks initiate at inhomogeneous sites specially on agglomeration particles of carbon black. Galeski [12], is of the opinion that during crystallization, the volume change creates micro-voids in a resin called weakness sites. These holes are stress concentration areas where micro-cracks initiate.

Fig. 20. Particles of catalytic residues in resins A and B.

Gedde [13] showed that during isothermal crystallization, macromolecules of low molecular weight segregate between spherolites and thicker lamellae. Segregation zones are probable paths of crack propagation.

In the present work, we have shown that creep damage is initiated on crystalline heterogeneous particles embedded in the matrix. These particles are catalytic residues. Nevertheless, loading of the structure induces a decohesion of the matrix at the surface of these particles whereas a stress concentration zone is formed in the surrounding material. Crazes are formed and SCG is initiated in the process zone.

So, catalytic residues seem to be the principal initiating factor to creep initiation of micro-cracks in our case. Other defects proposed by many authors could however cause secondary damages in the process zone (Fig. 23). These secondary micro-cracks can lead to dimples (see for example Fig. 16). Then the principal crack goes through those secondary damaged zones.

Even though the catalytic particles play an important role

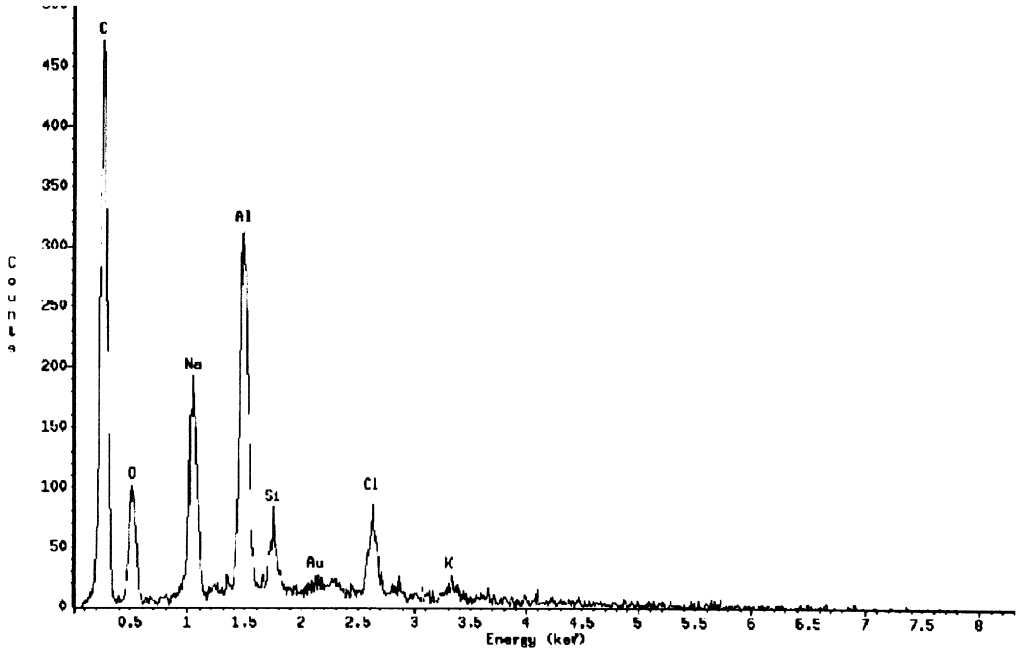

Fig. 21. Composition of catalytic residue (X microprobe analysis WDS).

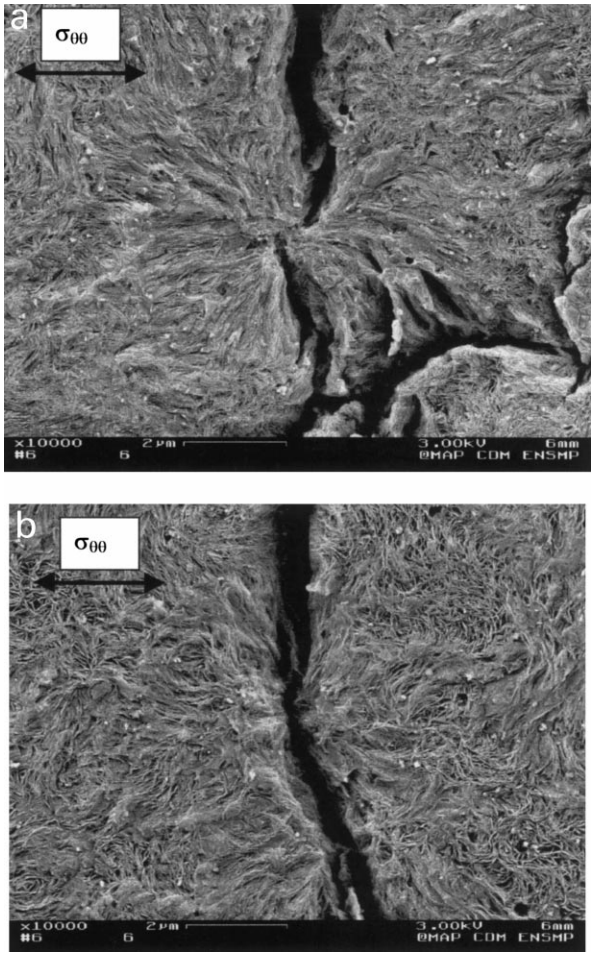

Fig. 22. Interlamellar propagation of creep micro-cracks in a transverse cross-section of a pipe (resin B).

in the initiation stage, their presence is not sufficient to initiate a SCG. In resin A, for example, we can detect the same kind of particles, but we cannot see any initiation of brittle failure causing SCG. The molecular microstructure of a polymer is an additional determinant factor for the formation of SCG. The volumic creep damage can be explained by the disentanglement mechanism of tie molecules as reported elsewhere [14].

In our case, resin A molecules have longer branching than resin B. This strongly suggests that entanglements in the amorphous zone should be more efficient whereas crystalline microstructure should be modified. Much more work is needed to answer the question. However, Bubeck and Baker [4] also reported that the length and side chain have an influence on the microstructure and physical properties of PE. The creep resistance increases as the length of the branches increases (methyl to hexyl) for a given density and molecular weight.

4.2. Intra-spherulitic creep crack propagation

Propagation can be both inter- [15] or intra-spherulitic [16] depending on the relative strength of the lamellae and of the spherulitic boundaries. In the present study, for resin B, Fig. 22 clearly shows that propagation occurs in the equatorial regions of the spherulite as predicted by Hay and Keller [17].

As a matter of fact, in this plane, the lamellae are perpendicular to the loading direction making the inter-lamellar separation, chain slipping and crystal rotation easier. Micro-cracks initiate in the process zone of a residue (Fig. 23) embedded in the spherulite and then propagate until they

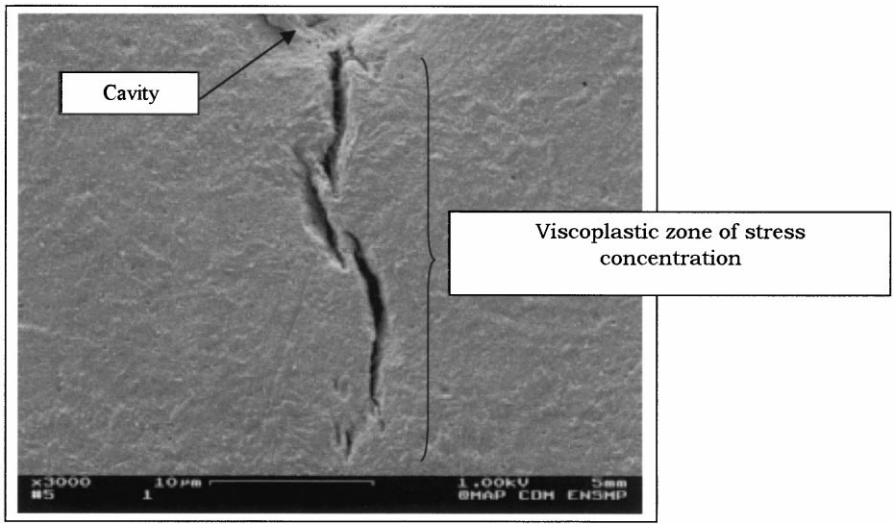

Fig. 23. Initiation and propagation of micro-cracks from a cavity around catalytic residues (resin B).

reach the spherulite center point where it can be deviated. When many spherulites are creep damaged, cracks may coalesce (Fig. 24).

The diagonal region of a spherulite is also a region susceptible to propagation [17]. In this region, crystalline lamellae are not only subjected to the normal stress, but also to shear stress activating crystalline slipping. This may explain the fact that micro-crack may change direction when going through the spherulite center (Fig. 22a). So, depending on the path of the crack, conical sections of spherulites (Fig. 15b) or plane sections of the fracture surface are observed (Fig. 15c). In all cases, the cracks propagate due to inter-lamellar mechanisms, essentially by fracturing tie molecules.

These inter-lamellar fracture mechanisms are also mentioned by many authors having mostly used ESC agents [1]. In that case Igepal is assumed to lubricate tie molecules and to accelerate creep failure. In our case, micro-crack goes through spherulites with almost no significant deformation. The interlamellar propagation at a submicronic scale produces a mirror-like fracture surface as earlier mentioned by Newman [18] in a typical fracture surface of polymethyl methacrylate.

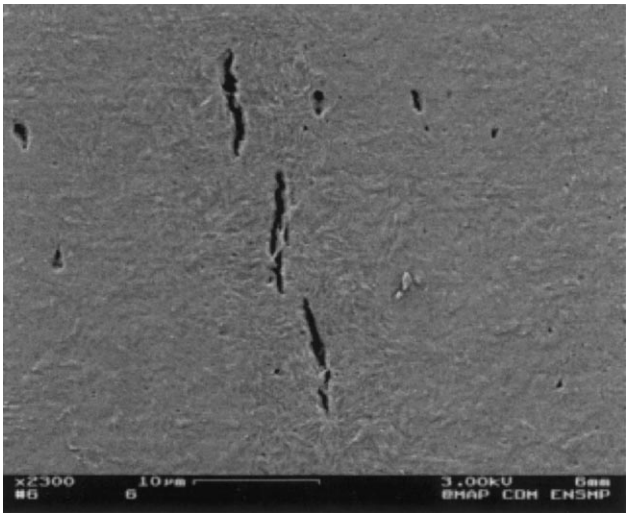

Fig. 24. Formation of cracks: coalescence stage (resin B).

Zandman [19], showed that the critical size of the mirror area (minimum size required to produce instability and SCG by discontinuous bands), decreases as the rate of loading increases. In our case (creep tests), the loading rate is very low. So the critical size only depends on the distance of the initiating cavity from the inner pipe wall surface (Fig. 25). In fact, when the mirror zone reaches this edge, the hoop stress opens the crack mouth and the crack tip blunts causing SCG by discontinuous bands.

Brittle failure can thus be seen as a rate-dependent process, i.e. low loading condition and long time lead to brittle fracture by allowing molecule disentanglement.

4.3. Creep crack growth by discontinuous bands

Both Lustiger and Corneliussen [6] and Lu et al. [7,8] used a single edge notched specimen (SENT) in tension to study SCG in MDPE. In this work, we chose a full notched axisymmetrical specimen (see Fig. 6) and show that SCG also occurs in these conditions.

The geometric features of discontinuous crack growth such as the spacing between the arrest lines and the height of the fibrillated structure increases with temperature and stress. Lu explained these facts in the framework of the Dugdale theory [8]. According to our observations, a crazing criterion seems to be more accurate to study SCG than a yield one.

The secondary crazes, that are formed at about 45°, are mainly produced by the shear component of the stress field. They tend to increase the time of the crack arrest by relaxing the local stress.

Besides these "usual" observations our work emphasizes

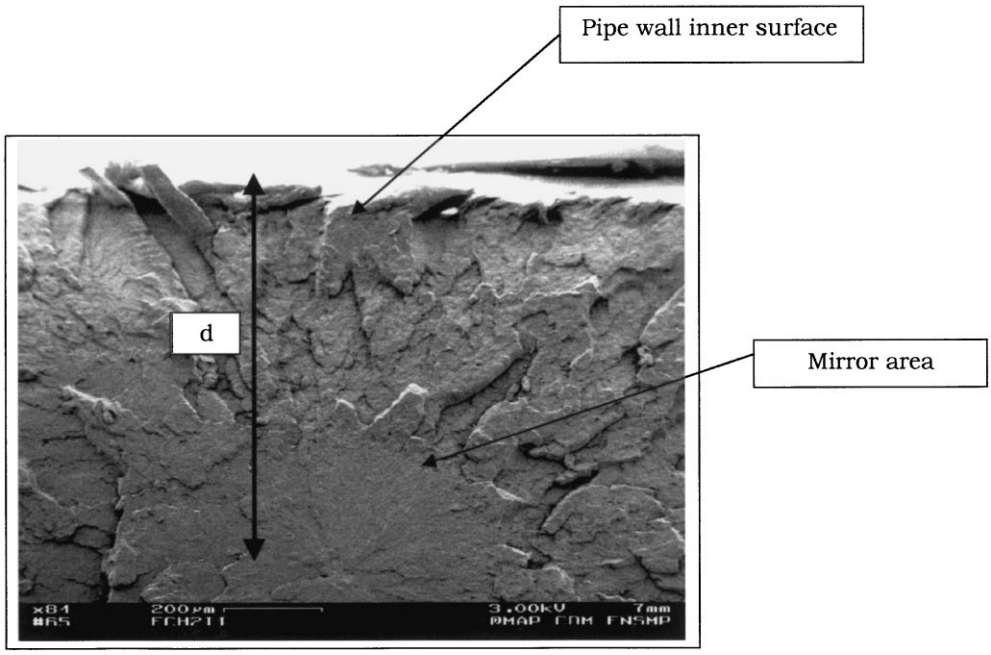

Fig. 25. Localization of the creep damage initiation site near the pipe wall inner surface (resin B).

the existence of a volumic creep damage in the whole pipe wall which leads to an equivalent damage process and to the final fracture of the pipe, but without pre-crack initiation. In the first stage, a mirror area appears around the initiating cavity. Transition occurs when propagation reaches the inner edge of the pipe wall. Propagation then continues by discontinuous bands creating a fibrillated fracture surface.

5. Conclusions

Our observation allows us to conclude that:

- Catalytic residues are an initiating factor of creep damage, but their presence is not sufficient to generate an SCG in PE. The nature of the PE matrix is a predominant factor.
- SCG occurs in both pre-cracked and uncracked specimens.
- MDPE can be creep damaged in its whole volume.
- Volumic creep damage can initiate and propagate a creep crack by discontinuous bands up to the final brittle fracture.
- For an MDPE pipe, creep damage is inter-lamellar and the cracks propagate by disentanglement of tie molecules through the spherulites making up a mirror-like fracture surface. When this internal damage emerges at the inner tube surface, crack propagates by discontinuous bands creating a fibrillated fracture surface.
- Laboratory specimens are notched, so crack propagates by discontinuous bands (no initiating mirror area).

Acknowledgements

Financial support from Gaz de France (GDF) is gratefully acknowledged.

References

[1] Singleton CJ, Roche E, Geil PH. J Appl Polym Sci 1977;21:2319–40.
[2] Chan MKV, Williams JG. Polymer 1983;24:234.
[3] Lu X, Brown N. J Mater Sci 1986;21:2423.
[4] Bubeck RA, Baker HM. Polymer 1982;23:1680–4.
[5] Leis B, Ahmed J, Forte T, Hulbert L, Wilson M. Investigation of the validity of the slow crack growth test. GRI Report No. 88/O131, May 1988 (draft).
[6] Lustiger A, Corneliussen RD. J Mater Sci 1987;22:2470–6.
[7] Lu X, Brown N. J Mater Sci 1991;26:612–20.
[8] Lu X, Qian R, Brown N. J Mater Sci 1991;26:917–24.
[9] Ward AL, Lu X, Huang Y, Brown N. Polymer 1991;32:2172–8.
[10] Lu X, Brown N. J Mater Sci 1990;25:411–6.
[11] Stockmayer P, Wintergerst S. 3R Int. 1981;20:274.
[12] Galeski A, Piorkowiska E. J Polym Sci 1983;21:1313–22.
[13] Gedde UW, Jansson JF. Polymer 1985;26:1469–76.
[14] Lu X, McGhie A, Brown N. J Polym Sci: Part B 1992;30:1207–14.
[15] Bandyopathyay S, Brown HR. Polymer 1978;19:589–92.
[16] Butler MF, Donald AM. J Mater Sci 1997;32:3675–85.
[17] Hay IL, Keller A. Kolloid -Z. Z. Polym 1965;204:43.
[18] Wolock I, Kies JA, Newman EB. In: Averbach BL, editor. Fracture. New York: Wiley, 1959. p. 250.
[19] Zandman F. Etude de la Déformation et de la Rupture des Matières plastiques. Publications Scientifiques et Techniques du Ministère de l'Air, Paris, France, 1954.